The Effect on Retinal Structure and Function of 15 Specific *ABCA4* Mutations: A Detailed Examination of 82 Hemizygous Patients

Ana Fakin,[1,2] Anthony G. Robson,[1,2] John (Pei-Wen) Chiang,[3] Kaoru Fujinami,[1,2,4,5] Anthony T. Moore,[1,2,6] Michel Michaelides,[1,2] Graham E. Holder,[1,2] and Andrew R. Webster[1,2]

[1]Institute of Ophthalmology, University College London, London, United Kingdom
[2]Moorfields Eye Hospital, London, United Kingdom
[3]Casey Molecular Diagnostic Laboratory, Portland, Oregon, United States
[4]National Institute of Sensory Organs, National Hospital Organization, Tokyo Medical Center, Tokyo, Japan
[5]Department of Ophthalmology, Keio University, School of Medicine, Tokyo, Japan
[6]Department of Ophthalmology, University of California-San Francisco School of Medicine, San Francisco, California, United States

Correspondence: Andrew R. Webster, UCL Institute of Ophthalmology, 11-43 Bath Street, London EC1V 9EL, England; andrew.webster@ucl.ac.uk.

Submitted: August 2, 2016
Accepted: September 22, 2016

Citation: Fakin A, Robson AG, Chiang J(P-W), et al. The effect on retinal structure and function of 15 specific *ABCA4* mutations: a detailed examination of 82 hemizygous patients. *Invest Ophthalmol Vis Sci*. 2016;57:5963–5973. DOI:10.1167/iovs.16-20446

Purpose. To determine the effect of 15 individual *ABCA4* mutations on disease severity.

Methods. Eighty-two patients harboring 15 distinct *ABCA4* mutations in trans with null (hemizygous), 10 homozygous, and 20 nullizygous patients were recruited. Age of onset was determined from medical histories. Electroretinography (ERG) responses were classified into three groups (normal; cone dysfunction; cone and rod dysfunction). The dark-adapted bright-flash (DA 10.0) a-wave amplitudes and the light-adapted flicker ERG (LA 3.0 30 Hz) amplitudes were plotted against age and compared with the nullizygous patients. Fundus autofluorescence imaging (FAF) was assessed when available.

Results. Patients hemizygous for p.G1961E and p.R2030Q had normal ERGs. Patients harboring p.R24H, p.R212C, p.G863A/delG, p.R1108C, p.P1380L, p.L2027F, and c.5714+5G>A had abnormal ERGs (ERG group 2 or 3) at older ages, in most cases with significantly higher amplitudes than nullizygous patients. Mutations p.L541P+A1038V, p.E1022K, p.C1490Y, p.E1087K, p.T1526M, and p.C2150Y were associated with abnormal ERGs (group 2 or 3) and amplitudes comparable to those of nullizygous patients. The majority of patients, including those harboring p.G1961E, had foveal atrophy; while both patients harboring p.R2030Q had foveal sparing. Most patients harboring intermediate and null-like mutations displayed FAF abnormalities extending beyond the vascular arcades.

Conclusions. In the hemizygous state, 2/15 *ABCA4* alleles retain preserved peripheral retinal function; 7/15 are associated with either preserved or only mildly abnormal retinal function, worse in older patients; 6/15 behave like null mutations. These data help characterize the degree of dysfunction conferred by specific mutant ABCA4 proteins in the human retina.

Keywords: ABCA4, retinal dystrophy, electrophysiology, inherited retinal disease, fundus autofluorescence

Biallelic mutation of the *ABCA4* gene is the most common cause of inherited retinal disease, leading to significant permanent blindness in many affected people.[1–4] In the era of emerging therapies for genetically determined disease, it is critical in the design and interpretation of intervention trials to understand the natural history and the causes of disease variability. Several in vitro and animal studies investigating the effects of various *ABCA4* mutations have been performed,[5–12] but clinical phenotypic correlations have not yet been established for most. Retinal disease caused by *ABCA4* mutations includes phenotypes such as early-onset cone–rod dystrophy, limited macular dystrophy, and late-onset foveal sparing disease. Attempts at establishing genotype–phenotype correlations in humans have been hindered by age-related differences in phenotype, vast allelic heterogeneity, and the fact that the combined effects of two alleles, not one, determine the clinical presentation in affected people.[13–15] This study partly surmounts the complexity by studying those with a genotype in which one of the two alleles is an established "null" allele, allowing the clinical effect of the remaining allele to be determined unambiguously. We use a robust objective measure of the peripheral retinal function, the electroretinogram (ERG), and fundus autofluorescence (FAF) imaging of the macula to study the effect of 15 different *ABCA4* alleles.

Methods

Patient Selection

The data derive from 82 patients (46% male, median age 31 years; range 9–75) harboring one of 15 different *ABCA4* mutations (Table 1) in trans with a null mutation (referred to as hemizygous for the purpose of this paper). A further cohort of 20 patients, harboring two null mutations in trans

Table 1. Number of Included Patients for Each of the Studied *ABCA4* Mutations

Mutation		*n*	
Base Change	**Amino Acid Change**	**Hemizygous**	**Homozygous**
c.5882G>A	p.G1961E	23	NA
c.2588G>C	p.G863A/delG*	19	NA
c.1906C>T	p.L2027F	9	NA
c.6449G>A	p.C2150Y	6	NA
c.5714+5G>A†	Splice-site mutation	5	NA
c.71G>A	p.R24H	3	NA
c.6089G>A	p.R2030Q	2	NA
c.634C>T	p.R212C	3	2‡
c.4577C>T	p.T1526M	3	2
c.3322C>T	p.R1108C	2	1
c.3064G>A	p.E1022K	1	2
c.4139C>T	p.P1380L	2	1
c.4469G>A	p.C1490Y	2	1
c.3259G>A	p.E1087K	1	1
c.1622T>C+c.3113C>T complex allele	p.L541P+p.A1038V complex allele	1	/
Total		82	10
Nullizygous		20, plus 1 without ERG data	

* c.2588G>C is associated with two different protein products in approximately equal ratios, glycine-to-alanine substitution at codon 863 (p.G863A) and removal of codon 863 due to an activation of a cryptic splice acceptor site in exon 17 (p.G863del),[13] and is, for the purpose of this study, referred to as p.G863A.

† c.5714+5G>A has been shown to result in a mixture of normally and abnormally spliced ABCA4 protein.[20]

‡ The patients were included in a previous paper.[21]

(nullizygous), were examined in parallel (60% male, median age 12 years; range, 6–40) and used for comparison, and one nullizygous patient without ERG data was recruited for FAF comparison in his age group. All patients were recruited from a cohort of 488 genetically confirmed patients with ABCA4-retinopathy. Mutations were included if there was at least one hemizygous patient with ERG data. If the phenotype was mild at a young age (normal ERG at age < 20 years), there had to be at least one older patient with the same mutation (>40 years) in an attempt to assess possible ERG deterioration with age. In addition, for mutations associated with severe phenotypes, a cohort of homozygous patients ($n = 10$) was reviewed in order to examine the clinical effect of doubled allele dosage. That is, the clinical consequence of a missense allele behaving like a null would be comparable in the hemi- and homozygous states, whereas one with residual function might be expected to show an improved clinical outcome when homozygous, where gene dosage is twice that of a hemizygote. For the purpose of this study, mutation was considered to be null if it was either a stop mutation, a frame-shifting mutation resulting in a stop codon, predicted to undergo nonsense-mediated decay,[16] or a splicing mutation previously shown to behave as null, that is, c.5461-10T>C[17] or c.6729+4del15.[18] Other splice-site mutations, including those in the canonical regions, were excluded to minimize the potential effects of leaky splicing.[19] The genotypic data appear in Supplementary Table S1. The 15 mutations studied here accounted for 36% (349) and the null mutations for 27% (261) of the 976 disease-associated alleles of the total patient cohort.

Clinical Assessment

Disease onset was defined as the age when patients first noticed visual problems. Electroretinography (ERG) incorporated the recommendations of the International Society for Clinical Electrophysiology of Vision (ISCEV).[22] The pattern ERG, reflecting macular function, was indistinguishable from noise in the majority of patients (data not shown). These data were not, therefore considered in this study. Full-field ERG responses were detectable in most, and were used to study the degree of peripheral retinal dysfunction. Patients were classified by experienced electrophysiologists (GEH, AGR) into one of three ERG groups[23]: normal (group 1; dysfunction confined to the macula), generalized cone system dysfunction (group 2), or cone and rod system dysfunction (group 3). Age at ERG examination, age at onset, ERG group, and genotype for each patient are shown in Supplementary Table S1. The data showed a high degree of interocular symmetry, and right eye data were used for analysis. Fundus autofluorescence and optical coherence tomography (OCT; Spectralis, Heidelberg, Germany) were assessed when available (76/82 patients).

Categorizing *ABCA4* Mutations

The clinical impact of the different *ABCA4* mutations was determined using ERGs in the following steps. (1) The proportion of patients with group 1 ERG was determined for each genotype, and on the basis of that, the categories of mild, intermediate, and null-like mutations were established. (2) In order to confirm that the categories had clearly separate amplitude progression patterns and to further subclassify the intermediate category, the DA 10.0 (dark adapted; ERG to flash strength of 10.0 cd.s.m^{-2}) a-wave amplitudes were plotted against age and compared with a regression line fitting equivalent measurements in nullizygous patients (where the line's 95% confidence interval was used to detect a significant difference). The LA 3.0 30-Hz (light-adapted ERG, flash strength 3.0 cd.s.m^{-2} presented at 30 Hz) amplitude was analyzed in a similar manner; other ISCEV Standard ERG parameters were analyzed as a supportive measure. (3) Homozygous patients were assessed for mutations associated with the most severe phenotypes to determine whether the addition of a further identical allele resulted in a milder phenotype. The relationship between amplitude and peak time of DA 10.0 a-wave and LA 3.0 30 Hz was explored in patients with abnormal ERGs, to determine whether any of the mutations produced a different mode of disease progression (e.g., peak time change prior to amplitude loss or vice versa).

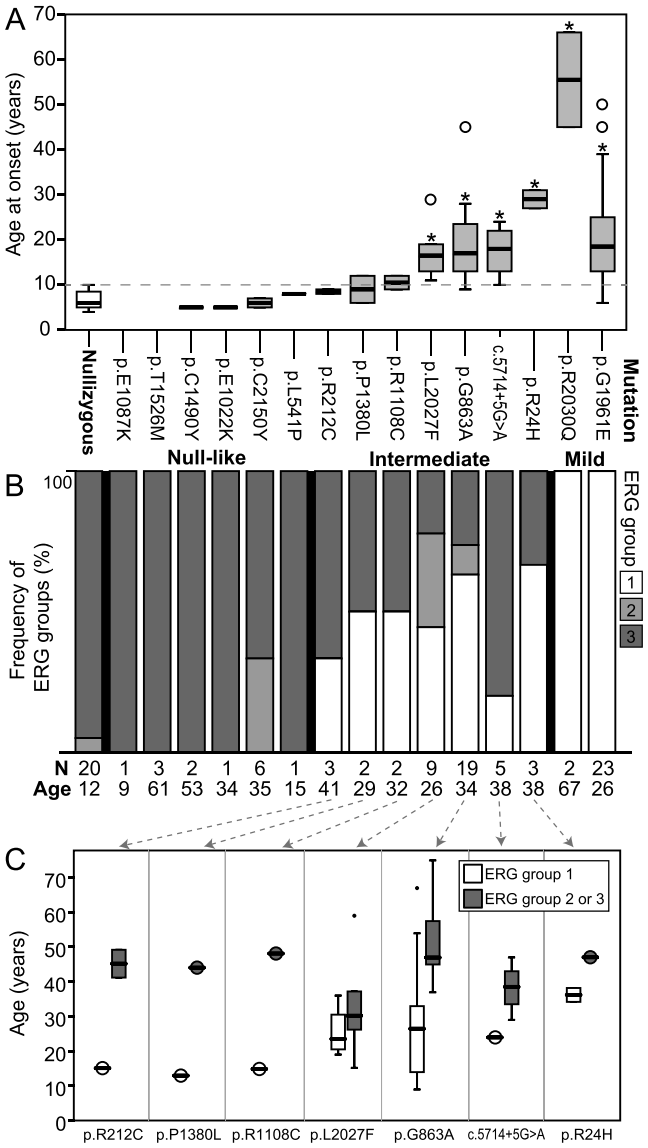

Figure 1. (**A**) Box plot chart showing the distribution of ages of onset of visual symptoms for different genotypes. Mutations (all in trans with null) are marked *below each box plot*. Significantly delayed onset in comparison to the nullizygous group is marked by *asterisks* (Mann-Whitney U test, $P < 0.05$). *Dashed line* represents the latest age of onset observed in the nullizygous group. (**B**) Frequency of different ERG groups for each mutation. The median ages of patients for each of the studied mutations are noted *below the columns*. (**C**) Box plot chart showing the age distribution of patients harboring the intermediate mutations, separately for patients with normal (ERG group 1) and abnormal (ERG group 2 or 3) ERG. For each mutation the median age of patients with normal ERG was lower than the median age of patients with abnormal ERG. *Circular symbols* represent single cases.

The ERG data from 137 healthy controls ($n = 137$)[24,25] were plotted on all charts as reference for the normal age-related change in ERG amplitudes.

Genetic Analysis

The majority of genotypes were ascertained by next-generation sequencing as a part of retinal panel at Casey Eye Institute. Specifically, direct testing for mutations in the genes of the Stargardt/Macular dystrophy SmartPanel v4 (613 primer sets) was performed by PCR amplification and next-generation sequencing. Polymerase chain reaction primer sets were printed onto a specific chip. Each primer set is duplicated on the chips in order to avoid random PCR failure. Any low-coverage region (<100×) was covered afterward by PCR and Sanger sequencing. Identified mutations and novel variations were confirmed by Sanger sequencing. All exons and exon/intron boundaries were sequenced. Exon 1 is defined as the exon having the start codon ATG. Codon 1 corresponds to the start ATG and nucleotide 1 to the A. The canonical *ABCA4* transcript sequence, ENST00000370225, was used to compare exonic sequence. Phase of the two variants was explored in the majority of patients (when the relatives were available), and in each case they were in trans. When segregation was not possible, the variants were assumed to be in trans if (1) phenotype was consistent with ABCA4-retinopathy; (2) the patient had exactly two *ABCA4* mutations (with complex allele p.L541P+p.A1038V counting as one); and (3) the two *ABCA4* mutations were not previously reported in cis in a complex allele. All included patients met those criteria.

Statistical Analysis

Statistical analysis was performed using SPSS software v. 22 (IBM SPSS Statistics, IBM Corporation, Chicago, IL, USA). The Mann-Whitney U test was used to test for significant differences in median age of onset between the patients, hemizygous for each of the studied mutations, and the nullizygous group. The 95% confidence interval of the nullizygous regression line was used to determine whether the ERG amplitudes of the hemizygous patients differed significantly from those of the nullizygous patients. Fisher's exact test was used to compare the frequencies of an abnormal ERG among different genotypes associated with widespread FAF abnormalities.

Institutional Review Board (IRB)/Ethics Committee approval was obtained. The research adhered to the tenets of the Declaration of Helsinki.

Results

Age of Disease Onset

Six mutations (c.5714+5G>A, p.R24H, p.G863A, p.G1961E, p.L2027F, and p.R2030Q) had significantly later median ages of onset (Mann-Whitney U test, $P < 0.05$) compared to the nullizygous group, while seven mutations (p.R212C, p.L541P+A1038V, p.E1022K, p.R1108C, p.P1380L, p.C1490Y, and p.C2150Y) were comparable to the nullizygous group (Fig. 1A); onset data were not available for p.E1087K and p.T1526M.

Electroretinography

A summary of the main ERG parameters for each of the studied mutations appears in Supplementary Table S2. Figure 1B shows the frequency of different ERG groups for each of the studied mutations. Two mutations were consistently associated with normal (group 1) ERGs, and six mutations were consistently associated with abnormal ERGs (group 2 or 3). Seven mutations could be associated with either normal or abnormal ERGs. The age distribution analysis of the latter revealed a tendency toward a normal ERG at younger ages and abnormal ERG at older ages (Fig. 1C), but the number of patients was too low for statistical analysis. None of the mutations was exclusively associated with ERG group 2. Patients with ERG group 2 were further explored in terms of age and disease duration (Supplementary Fig. S1). Within each genotype, the age and/or disease duration of those patients fell between

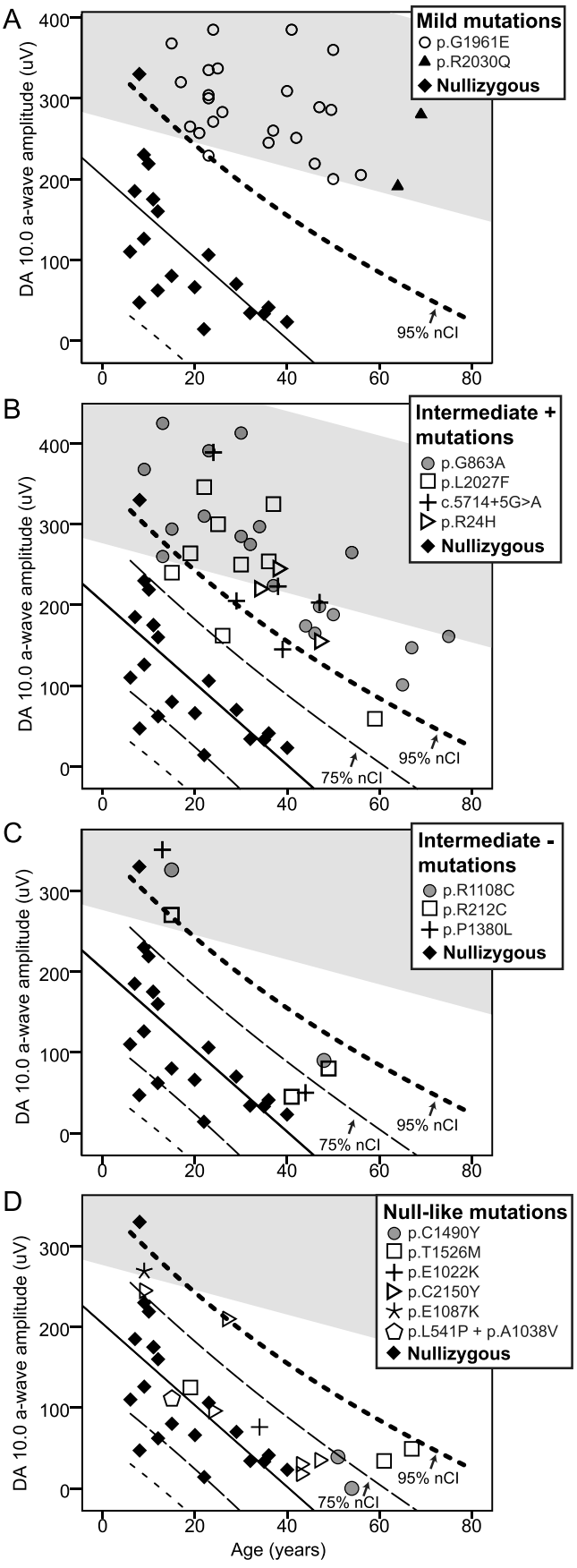

Figure 2. The DA 10.0 (dark adapted; ERG to flash strength of 10.0 cd.s.m^{-2}) a-wave amplitudes of patients hemizygous for 15 different *ABCA4* mutations, plotted by age. Mutations of similar severity are divided into four groups and shown separately. The *gray area* represents the 95% confidence interval of the healthy volunteers. On each chart the nullizygous patients are shown as a baseline reference with their regression line and its confidence intervals. (**A**) Mutations consistently associated with normal ERG (ERG group 1). (**B**) Mutations resulting in abnormal ERG at older ages, with amplitudes significantly better than those of the nullizygous patients in most cases. (**C**) Mutations resulting in abnormal ERG at older ages, with amplitudes comparable with those of the nullizygous patients. (**D**) Mutations consistently associated with abnormal ERG (ERG group 3) with amplitudes comparable to those of the nullizygous patients.

those in ERG groups 1 and 3, but the low number of patients precluded statistical analysis.

The plots of DA 10.0 a-wave amplitudes against age show that patients hemizygous for p.G1961E or p.R2030Q had significantly better amplitudes than nullizygous patients in all cases (Fig. 2A) and were thus classified as mild. In contrast, none of the patients hemizygous for p.E1022K, p.E1087K, p.C1490Y, p.T1526M, p.C2150Y, or p.L541P+A1038V had significantly better amplitudes than nullizygous patients (Fig. 2D), and were thus classified as null-like. The majority of patients hemizygous for c.5714+5G>A, p.R24H, p.G863A, or p.L2027F had significantly better amplitudes than nullizygous patients, even in cases where the ERG amplitudes were subnormal (mostly older patients) (Fig. 2B). Patients hemizygous for R212C, p.R1108C, or p.P1380L had significantly better amplitudes at younger (<20 years) but not older ages (>40 years; Fig. 2C). The latter two groups are thus classified as intermediate+ and intermediate−.

Analysis of other ERG parameters was largely consistent with these findings (Fig. 3; Supplementary Fig. S2; Supplementary Table S2). None of the mutations was notably different from the others in terms of the relationship between amplitude loss and peak time delay (Supplementary Fig. S4). Analysis of ERG amplitudes against disease duration was also performed, with consistent results; age was chosen as the main parameter for classification because of a larger set of available data and the ability to consider age-related normative data (Supplementary Fig S3).

Mutations resulting in severe ERG phenotypes were assessed in homozygous states, when available (Fig. 4). Patients homozygous for p.R212C, p.R1108C, and p.P1380L had significantly better amplitudes in comparison to the equivalent hemizygous patients (Fig. 4A), whereas patients homozygous for E1022K, p.E1087K, p.C1490Y, and p.T1526M were still similar to nulls (Fig. 4C). The analysis of the LA 3.0 30-Hz amplitudes was consistent with these findings with the exception of p.T1526M (Supplementary Fig. S2).

Fundus Autofluorescence and Optical Coherence Tomography

The structural changes in the macula were assessed using FAF and OCT for each severity class after classifying the mutations by ERGs (Supplementary Table S3; Fig. 5). Two distinct phenotypes were observed for the mild mutations p.G1961E and p.R2030Q. The majority of p.G1961E patients had a notable loss of photoreceptors in the fovea, and flecks were either absent or localized within the vascular arcades, while both p.R2030Q patients had foveal sparing and widespread flecks and mottling in the macula and extending beyond the vascular arcades (representative OCT images shown in Fig. 5). Intermediate mutations displayed a relatively homogenous phenotype for all genotypes, with the fundus abnormalities extending beyond the vascular arcades in 85% (34/40) of cases. In the early stages, patients often exhibited a relatively small

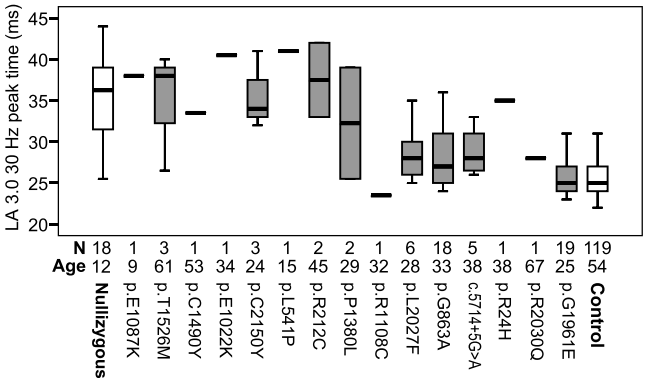

Figure 3. Box plot chart showing the distribution of LA 3.0 30-Hz peak times for each of the studied mutations. Nullizygous and control data are shown for reference. Mutations are arranged in the same order as in Figure 1 (according to increasing age at disease onset, with exception of p.G1961E). Number of patients with available data and their median age are shown for each of the mutations.

central atrophic lesion, surrounded by widespread flecks (other than patients harboring intermediate p.R212C and p.P1380L), often associated with a normal ERG (Fig. 5, second column), while at the later stages the central atrophy was larger and surrounded with widespread RPE mottling, and usually associated with ERG group 2 or 3 (Fig. 5, third column). There were three patients with foveal sparing, harboring p.R24H, p.G863A, and p.L2027F (ages 34, 54, and 22 years, respectively), all with normal ERGs. For the mutations p.R212C, p.R1108C, and p.P1380L (classified as intermediate–), the age-matched homozygous patients all showed notably greater RPE preservation outside the vascular arcades (Fig. 4C). Null-like mutations were associated with foveal atrophy in all cases and widespread FAF abnormalities, qualitatively similar to the age-matched nullizygous phenotypes (Fig. 5). Flecks were present only in the youngest patients, while large areas of central atrophy and widespread mottling were observed at older ages. Homozygous patients (available for p.E1022K, p.E1087K, p.C1490Y, and p.T1526M) exhibited similarly severe phenotypes (Fig. 4D). Figure 6 shows representative OCT scans through the flecks associated with intermediate and null mutations. The flecks in all cases examined were located at the RPE level, but there was better preservation of photoreceptor layers surrounding the flecks in patients harboring intermediate mutations (Fig. 6B–D). The association between FAF abnormalities and abnormal ERG was strongly dependent on the genotype. Among patients with widespread FAF irregularities, an abnormal ERG was observed in 0%, 66%, and 100% cases for mild, intermediate, and null-like mutations, respectively (significant for all intergroup comparisons, Fisher's exact test, $P < 0.005$).

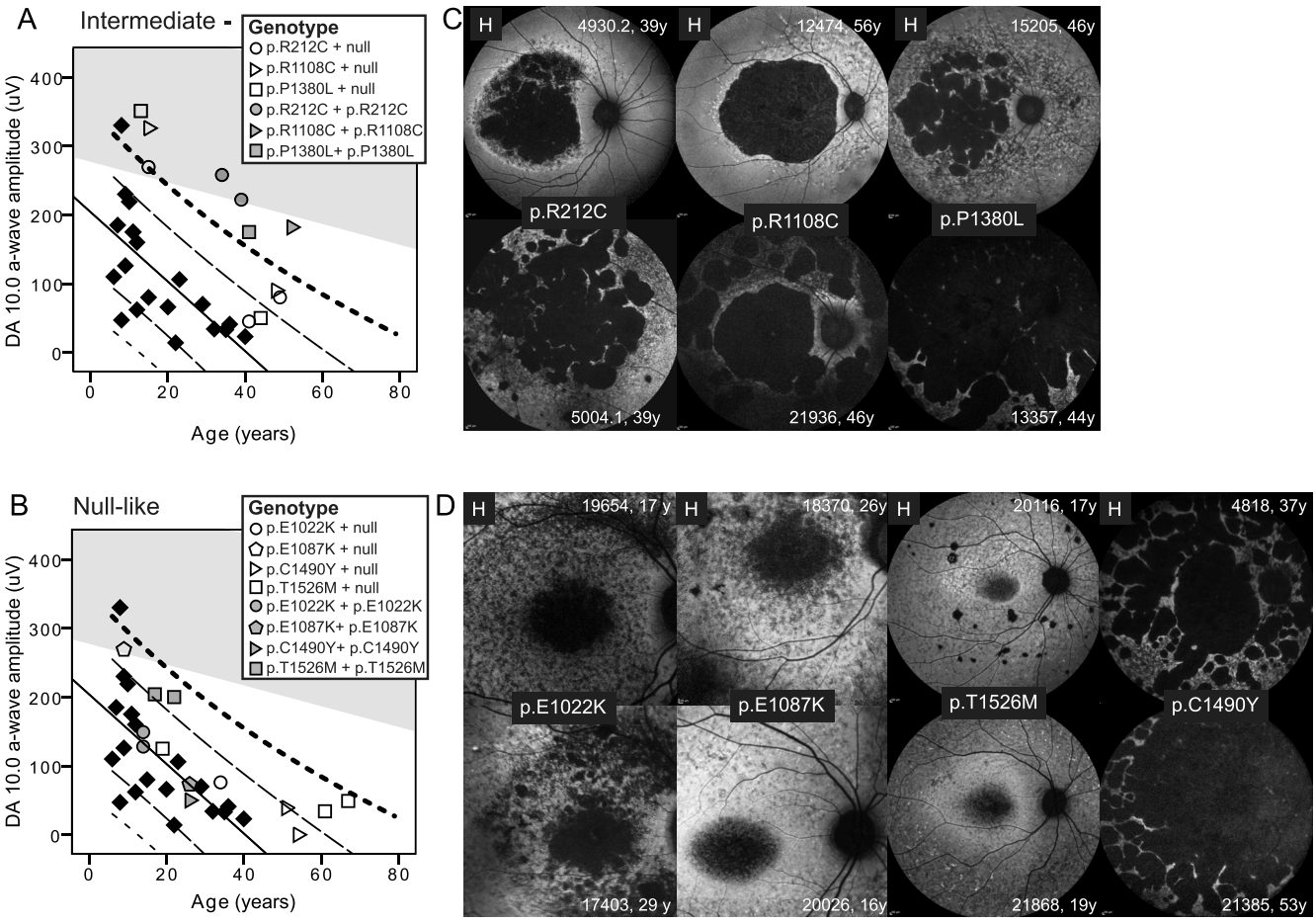

Figure 4. Comparison of ERG and FAF of patients hemizygous or homozygous for the same mutation. Mutations p.R212C, p.P1380L, and p.R1108C (**A**, **C**) were associated with a notably milder phenotype in homozygous states. Mutations p.E1022K, p.E1087K, p.T1526M, and p.C1490Y (**B**, **D**) displayed similarly severe phenotypes in hemizygous and in homozygous states. H, homozygous.

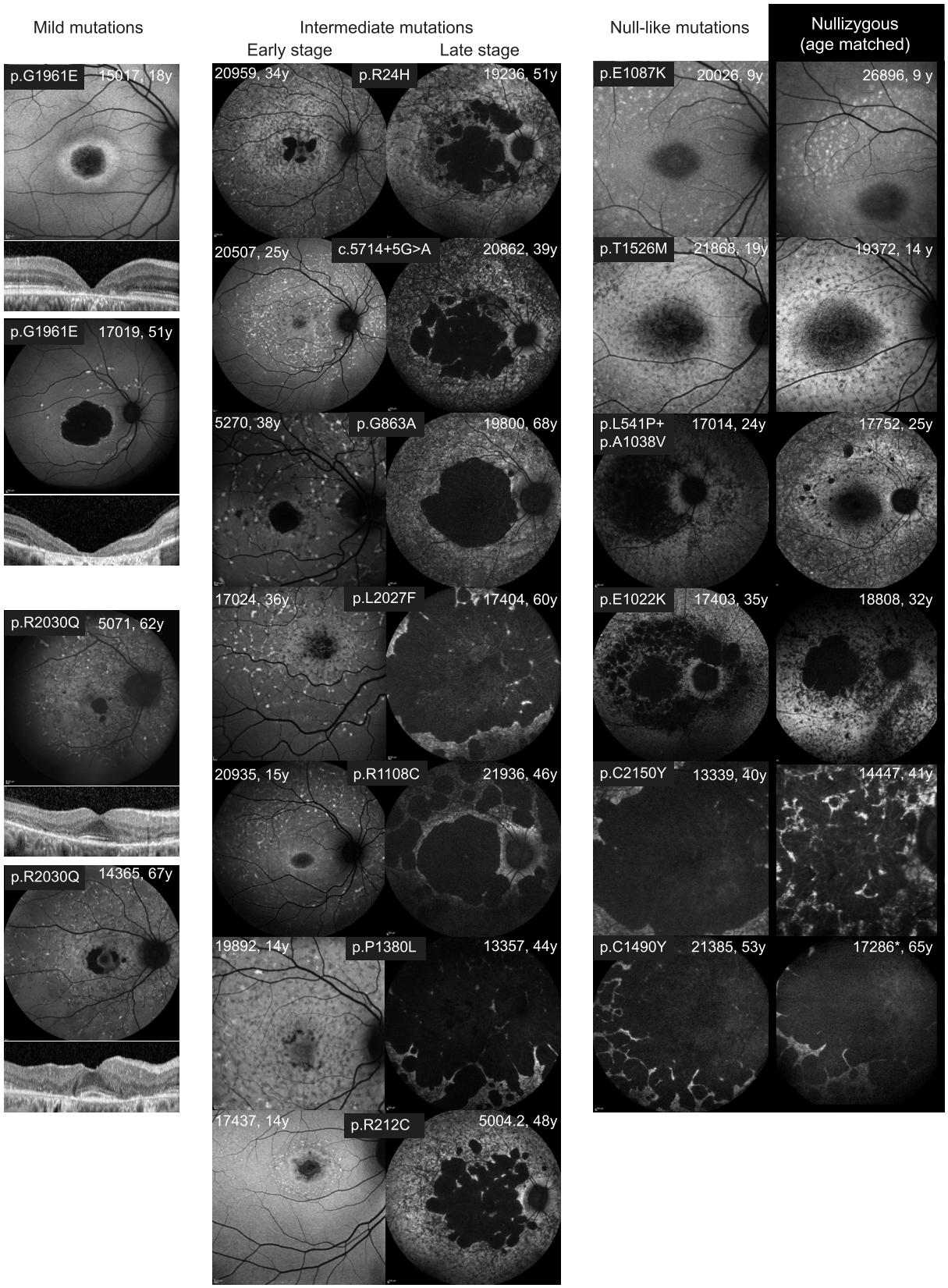

Figure 5. Representative fundus autofluorescence images of patients hemizygous for 15 different *ABCA4* mutations. Mutations of different ERG severity (mild, intermediate, and null-like) are shown in separate columns. Representative OCT scans are shown for p.G1961E and p.R2030Q to note the qualitatively different macular phenotypes (all had a normal ERG). A FAF image of a patient with a normal ERG (ERG group 1) and an abnormal ERG (ERG group 2 or 3) is shown for each intermediate mutation. An age-matched nullizygous patient is shown next to each nullizygous patient (all had an abnormal ERG).

Investigative Ophthalmology & Visual Science

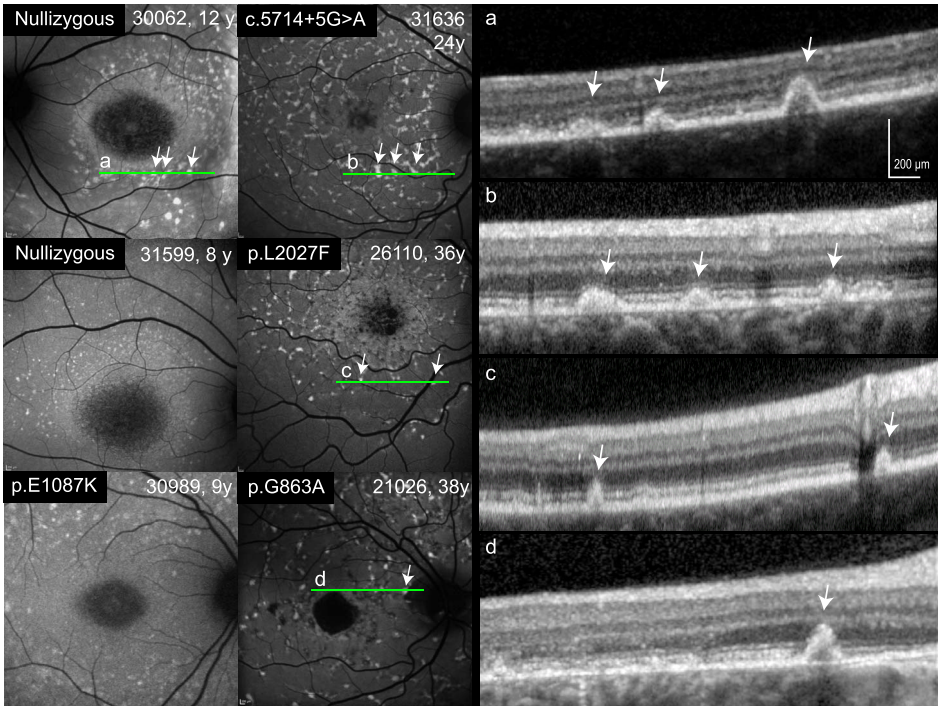

Figure 6. FAF and OCT characteristics of flecks (*arrows*) associated with null/null-like and intermediate alleles. Patient hemizygous for p.E1087K (null-like) mutation had qualitatively similar flecks to the nullizygous patients (*first column*), whereas the flecks of patients hemizygous for intermediate+ mutations were relatively larger and better delineated (*second column*). On the OCT scans (*third column*, location noted with *green lines*), the flecks of nullizygous and intermediate+ patients correlated with RPE thickening with no obvious qualitative differences in terms of their localization or shape (OCT of patients 31599 and 30989 were not available). However, the hyperreflective lines, representing photoreceptors (ISe and ELM), appeared to be more preserved in patients harboring intermediate+ mutations.

Discussion

Phenotypic Characteristics of Distinct *ABCA4* Mutations

This study proposes a categorization of 15 distinct *ABCA4* mutations into different severity classes based on the departures of their hemizygous phenotypes (when in trans with null) from the nullizygous phenotype. A summary of clinical findings and topographical location of the studied mutations are presented in Figure 7.

Mild Mutations (p.G1961E, p.R2030Q)

A mild phenotype associated with p.G1961E (normal ERGs, absence of dark choroid, and low quantitative FAF) has been reported previously,[26,27] but mostly in compound heterozygotes, carrying an additional missense mutation with an unknown effect. An important finding in the current study is that p.G1961E spares the peripheral retina when in a hemizygous state. Interestingly, the macular FAF pattern was different in the other mild mutation, p.R2030Q, causing a foveal sparing phenotype and extensive FAF irregularities. This corroborates reports on compound heterozygous patients, in which p.R2030Q was the most common mutation involved in foveal sparing,[28] and p.G1961E in the optical gap phenotype (i.e., isolated loss of photoreceptors in the fovea).[29] It will be important to use quantitative assessment of the FAF and OCT images to strengthen and expand these observations in the future. ABCA4-retinopathy is thought to be caused by at least two contributing pathogenic mechanisms, one being RPE damage triggered by phagocytosis of bisretinoid-laden outer segments, and the other being direct cone toxicity[12,30–32]; and it is tempting to speculate that the phenotypic differences between p.G1961E and p.R2030Q reflect the predilection for foveal cone damage for p.G1961E mutants and toward RPE damage for p.R2030Q mutants.

Intermediate Mutations (p.R24H, p.G863A, p.R1108c, p.P1380L, p.L2027F, c.5714+5G>A)

Intermediate mutations must produce a sufficient amount of functional ABCA4 protein to differentiate them from null; however, there is deterioration of peripheral retinal function with time. The FAF and OCT characteristics, that is, the presence of widespread flecks in patients with normal ERG and preserved photoreceptors surrounding the flecks on the OCT, suggest that the presence of ABCA4 function not only delays but may also modify the underlying pathophysiology of retinal degeneration, potentially causing prevalent RPE toxicity rather than direct photoreceptor toxicity. A quantitative analysis of FAF and OCT images is needed to explore this further. The p.G863A mutation is one of the most frequent *ABCA4* variants and was classified as mild in a previous study,[13] although only patients with a normal scotopic ERG were included, possibly skewing the genotype–phenotype correlation. The present study suggests that when in trans with a null, that mutation carries a considerable risk of retina-wide degeneration after the fourth decade, although it may be difficult to relay this information into clinical practice. There was a degree of intra- and interallelic phenotypic variability within the intermediate group. For example, the mutation p.R24H may be associated with the highest ABCA4 function within the group, as the patients had the latest median age at the onset of visual symptoms, and foveal sparing was present in the youngest patient. Conversely, p.R212C, p.R1108C, and p.P1380L mutations may be associated with the lowest degree

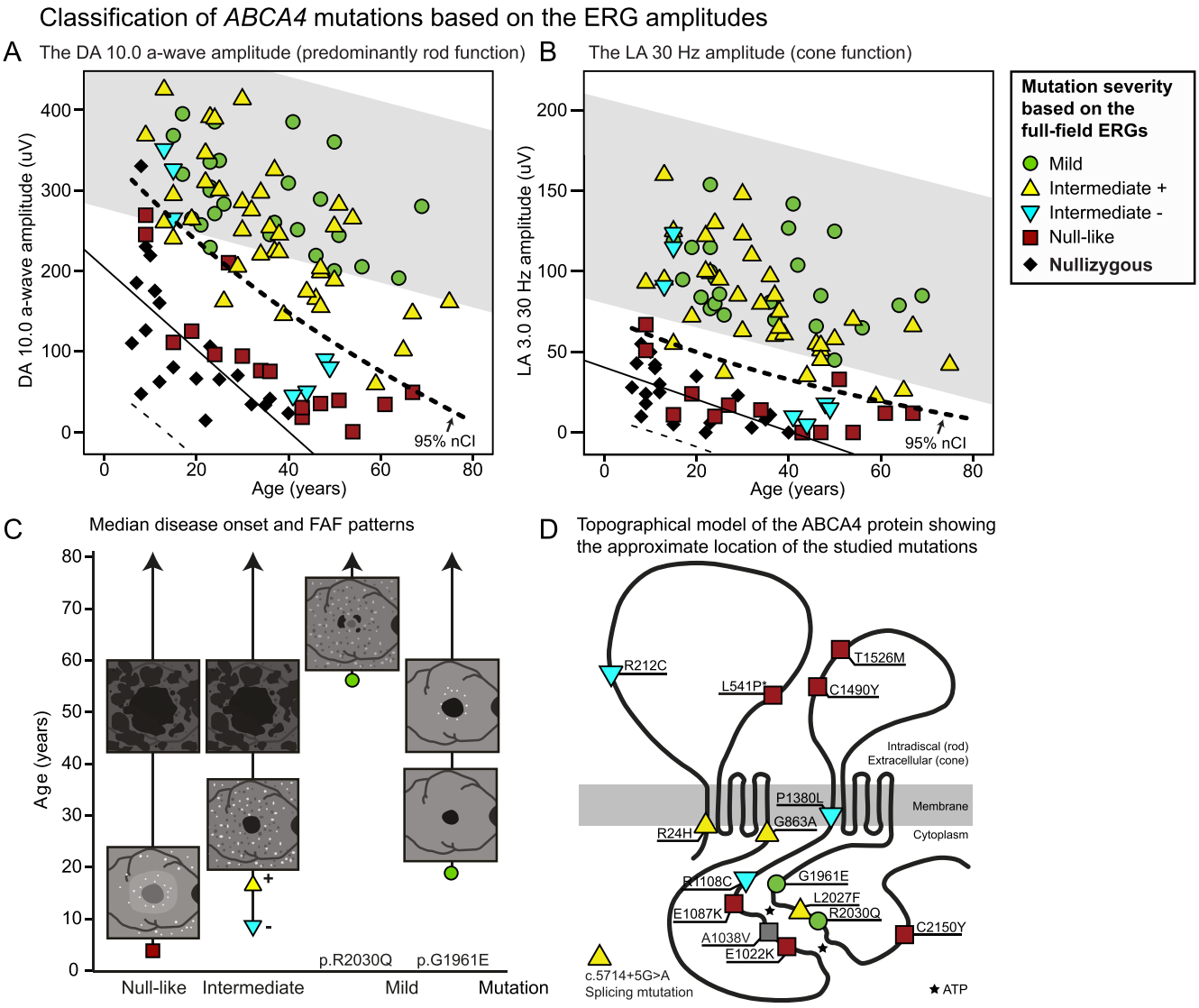

Figure 7. The DA 10.0 a-wave amplitudes (**A**) and the LA 3.0 30-Hz amplitudes (**B**) of 82 patients hemizygous for 15 different mutations, and 20 nullizygous patients, plotted by age. The severity of mutations based on the analysis of the DA 10.0 a-wave amplitudes is marked with different markers. The LA 30.0 30-Hz amplitudes were mostly consistent with the categorization. (**C**) Schematic representation of the median age of onset and FAF progression for different classes of mutations. Mutations p.R2030Q and p.G1961E, although both mild according to the ERG, displayed distinctly different FAF patterns. (**D**) Topographic model of ABCA4 protein showing the approximate location of the studied mutations. *For the complex allele p.L541P+p.A1038V, only the p.L541P is shown as *red* because it is considered the more pathogenic of the two based on previous studies.[10,11] Note the scale differences between charts A and B.

of ABCA4 function. They were the only three mutations from the intermediate group for which the median age of onset and the ERG amplitudes in the late stages did not differ significantly from the nullizygous group. Importantly, all three mutations displayed a milder phenotype in a homozygous state, suggesting a presence of some ABCA4 protein function.

Null-like Mutations (p.L541P+p.A1038V, p.E1022K, p.C1490Y, p.E1087K, p.T1526M, p.C2150Y)

The ages of onset, ERG amplitudes, and FAF abnormalities associated with null-like mutations were mostly comparable to those of the nullizygous patients. Ten of the studied mutations were previously included in one or both of the two larger genotype–phenotype studies to date[14,15] (Table 2), but those studies included compound heterozygotes and used subjective parameters of visual function such as visual field and visual acuity. Although direct comparison is difficult, there is general agreement regarding the severe phenotype associated with p.C2150Y and p.L541P+p.A1038V, and comparatively milder phenotype associated with p.G863A, p.P1380L, p.L2027F, p.R2030Q, and p.G1961E. There was some discrepancy regarding c.5714+5G>A, p.R1108C, and p.T1526M, which could reflect the phenotypic variability within a specific genotype and/or the fact that most patients in those studies harbored a second variant of unknown severity. It has been suggested that some *ABCA4* mutations, including p.L541P+p.A1038V (complex allele) and p.C2150Y, produce a more severe phenotype than the nullizygous genotype.[14] None of the mutations in the present study was associated with a more severe phenotype than seen in nullizygous patients, including p.C2150Y, represented by a considerable number of patients. There was, however, only one p.L541P+p.A1038V patient, and more data are needed to make a definitive conclusion regarding this allele. A limitation of the study is that analysis of the clinical impact of various hemizygous phenotypes cannot easily be extrapolated

Table 2. Classification of *ABCA4* Mutation on the Basis of ERGs

Severity Class/Mutation
Mild
p.G1961E[14,15]
p.R2030Q[14]
Intermediate+
p.R24H
p.G863A[13,15]
c.5714+5G>A[14,15]
p.L2027F[14,15]
Intermediate−
p.R212C
p.R1108C[15]
p.P1380L[14,15]
Null-like
p.L541P+A1038V[14,15]
p.E1022K
p.C1490Y
p.E1087K
p.T1526M[14]
p.C2150Y[14]

Mutations included in previous genotype–phenotype studies are noted with references.

to the more common situation in which the other mutation has some activity. Although the homozygous patients for intermediate− alleles provide some evidence that two non-null alleles could act in an additive manner, further studies are needed to address this question.

Correlations With Prior Observations of Specific Mutations

Review of in vitro observations, reported for p.G1961E, p.G863A, p.R1108C, p.P1380L, p.L2027F, p.L541P, p.A1038V, p.C1490Y, p.E1087K, and p.T1526M variants,[5–8,33] revealed several consistencies with the findings of the present study. Most mutations were studied using human embryonic kidney cell (HEK 293) cultures, allowing the assessment of the protein yield (although retained in the endoplasmic reticulum) and its affinity for adenosine triphosphatase (ATPase).[6] A subset of variants was additionally reconstituted into membranes and tested for basal and retinal-stimulated ATPase activities.[5,8,33]

Mild Mutations

The p.G1961E ABCA4 mutant in vitro exhibited an unusual ATPase activity profile in which the ATPase rate decreased with increasing concentrations of transretinal, the opposite to wild-type behavior, while its basal rate of ATPase activity was otherwise comparable to wild-type constructs.[6] The characteristic phenotype of p.G1961E patients, in which disease predominantly affects the fovea with little subsequent pathology elsewhere, might suggest that the need to respond to increasing transretinal concentration, over and above normal basal activity, might be a specific requirement of foveal cone photoreceptors.

Intermediate Mutations

The intermediate mutations p.G863A, p.R1108C, p.P1380L, and p.L2027F shared similar in vitro characteristics, showing a reduction in protein yields.[6] The splicing mutation c.5714+5G>A has also been shown to result in a decreased amount of (an otherwise normally spliced) product.[20] Functional experiments performed on p.G863A (for both the missense change and the deletion of glycine) revealed a reduction of basal ATPase activity but a preserved increase with increasing concentrations of transretinal, resembling the wild-type profile and opposite to that seen in p.G1961E, suggesting a biochemical correlate with the distinct clinical presentations.[6] Reduced protein yield of misfolded mutant peptides is due in part to their degradation by well-studied cellular quality control mechanisms.[34] An analogous phenomenon occurs in cystic fibrosis in which mutations of the gene *CTFR* cause perturbation of a related ABC transporter protein.[35] Clinical trials are in progress to assess the efficacy of a drug, VX-809, designed to reduced misfolding of specific mutants.[36] In vitro experiments have shown promising results (i.e., increased protein yields) for the same approach applied to *ABCA4* mutations p.R1108C and p.R1129C.[34] Other mutations from the intermediate group may also be candidates for testing the effect of such drugs.

Null-Like Mutations

The null-like mutations p.L541P+p.A1038V, p.C1490Y, p.E1087K, and p.T1526M shared similar in vitro characteristics in terms of producing near-normal protein yields[6,10] with varying degrees of ATPase dysfunction, in some cases similar to the in vitro profile of p.G1961E, which is surprising considering that they produced a severe, null-like phenotype. An important limitation of the studies using HEK 293 cells is the inability to demonstrate defects of protein localization that might be specific to the photoreceptor cells. Two of the mutations from this subgroup (p.C1490Y and p.L541P, but not p.A1038V) caused an almost complete mislocalization of the ABCA4 protein to the photoreceptor inner segments of transgenic frogs.[11] Although this was not duplicated in the p.L541P+p.A1038V transgenic mouse, in which the mutant protein seemed to be degraded,[10] a similar mechanism could be involved in pathogenesis in humans for those and other mutations from this severe subgroup.

An obvious limitation of this study is the small number of patients with some of the mutations, which was to some extent ameliorated by recruiting homozygous patients for those mutations. A further limitation was the difference in age of patients at the time of ERG recordings. This was to a large extent overcome by using the plots of ERG amplitudes against age and utilizing the amplitude decline of the nullizygous group as a baseline. Further longitudinal studies are nevertheless crucial to confirm these cross-sectional data. There was also variation in the phenotype seen within each of the studied genotypes, probably due to environmental or genetic modifier influencing the phenotype, and a certain extent of overlap between mutations of different classes of severity.

In conclusion, this study examines the effects of 15 *ABCA4* mutations, each occurring in trans with a null, on age of onset and on functional and structural retinal phenotypes. Quantified ERG parameters of rod and cone system function are compared with those of nullizygous *ABCA4* cases across a wide range of ages, identifying those likely to have residual function and enabling mutations to be graded into different severity classes. Additionally, the FAF patterns associated with those mutations are described, including the distinct p.G1961E phenotype, and the results interpreted in the context of in vitro studies to generate hypotheses of the disease mechanisms. The data inform our understanding of the effect of the genotype on the clinical presentation of ABCA4-retinopathy and may be helpful in the counseling and management of affected patients and

Investigative Ophthalmology & Visual Science

families, as well as in the optimum design and accurate interpretation of future interventional trials.

Acknowledgments

Supported by the National Institute for Health (NHS) Research Rare Diseases Translational Research Collaboration (NIHR RD-TRC, Cambridge, UK) and National Institute for Health Research (NIHR) Moorfields Biomedical Research Centre (London, UK), Institute of Ophthalmology, University College London (London, UK). The views expressed are those of the author(s) and not necessarily those of the NHS, the NIHR, or the Department of Health. The research has also been supported by Fight for Sight (London, UK) and Foundation Fighting Blindness (Columbia, MD, USA).

Disclosure: **A. Fakin**, None; **A.G. Robson**, None; **J.(P.-W.) Chiang**, None; **K. Fujinami**, None; **A.T. Moore**, None; **M. Michaelides**, None; **G.E. Holder**, None; **A.R. Webster**, None

References

1. Kitiratschky VB, Grau T, Bernd A, et al. ABCA4 gene analysis in patients with autosomal recessive cone and cone rod dystrophies. *Eur J Hum Genet*. 2008;16:812–819.
2. Riveiro-Alvarez R, Lopez-Martinez MA, Zernant J, et al. Outcome of ABCA4 disease-associated alleles in autosomal recessive retinal dystrophies: retrospective analysis in 420 Spanish families. *Ophthalmology*. 2013;120:2332–2337.
3. Maugeri A, Klevering BJ, Rohrschneider K, et al. Mutations in the ABCA4 (ABCR) gene are the major cause of autosomal recessive cone-rod dystrophy. *Am J Hum Genet*. 2000;67:960–966.
4. Hamel CP. Cone rod dystrophies. *Orphanet J Rare Dis*. 2007;2:7.
5. Suarez T, Biswas SB, Biswas EE. Biochemical defects in retina-specific human ATP binding cassette transporter nucleotide binding domain 1 mutants associated with macular degeneration. *J Biol Chem*. 2002;277:21759–21767.
6. Sun H, Smallwood PM, Nathans J. Biochemical defects in ABCR protein variants associated with human retinopathies. *Nat Genet*. 2000;26:242–246.
7. Biswas-Fiss EE. Functional analysis of genetic mutations in nucleotide binding domain 2 of the human retina specific ABC transporter. *Biochemistry*. 2003;42:10683–10696.
8. Biswas EE, Biswas SB. The C-terminal nucleotide binding domain of the human retinal ABCR protein is an adenosine triphosphatase. *Biochemistry*. 2000;39:15879–15886.
9. Biswas-Fiss EE, Affet S, Ha M, Biswas SB. Retinoid binding properties of nucleotide binding domain 1 of the Stargardt disease-associated ATP binding cassette (ABC) transporter ABCA4. *J Biol Chem*. 2012;287:44097–44107.
10. Zhang N, Tsybovsky Y, Kolesnikov AV, et al. Protein misfolding and the pathogenesis of ABCA4-associated retinal degenerations. *Hum Mol Genet*. 2015;24:3220–3237.
11. Wiszniewski W, Zaremba CM, Yatsenko AN, et al. ABCA4 mutations causing mislocalization are found frequently in patients with severe retinal dystrophies. *Hum Mol Genet*. 2005;14:2769–2778.
12. Conley SM, Cai X, Makkia R, Wu Y, Sparrow JR, Naash MI. Increased cone sensitivity to ABCA4 deficiency provides insight into macular vision loss in Stargardt's dystrophy. *Biochim Biophys Acta*. 2012;1822:1169–1179.
13. Maugeri A, van Driel MA, van de Pol DJ, et al. The 2588G→C mutation in the ABCR gene is a mild frequent founder mutation in the Western European population and allows the classification of ABCR mutations in patients with Stargardt disease. *Am J Hum Genet*. 1999;64:1024–1035.
14. Cideciyan AV, Swider M, Aleman TS, et al. ABCA4 disease progression and a proposed strategy for gene therapy. *Hum Mol Genet*. 2009;18:931–941.
15. Schindler EI, Nylen EL, Ko AC, et al. Deducing the pathogenic contribution of recessive ABCA4 alleles in an outbred population. *Hum Mol Genet*. 2010;19:3693–3701.
16. Zhang Z, Xin D, Wang P, et al. Noisy splicing, more than expression regulation, explains why some exons are subject to nonsense-mediated mRNA decay. *BMC Biol*. 2009;7:23.
17. Sangermano R, Bax NM, Bauwens M, et al. Photoreceptor progenitor mRNA analysis reveals exon skipping resulting from the ABCA4 c.5461-10T→C mutation in Stargardt disease. *Ophthalmology*. 2016;123:1375–1386.
18. Fakin A, Robson AG, Fujinami K, et al. Phenotype and progression of retinal degeneration associated with nullizigosity of ABCA4. *Invest Ophthalmol Vis Sci*. 2016;57:4668–4678.
19. Caminsky N, Mucaki EJ, Rogan PK. Interpretation of mRNA splicing mutations in genetic disease: review of the literature and guidelines for information-theoretical analysis. *F1000Res*. 2014;3:282.
20. Rivera A, White K, Stohr H, et al. A comprehensive survey of sequence variation in the ABCA4 (ABCR) gene in Stargardt disease and age-related macular degeneration. *Am J Hum Genet*. 2000;67:800–813.
21. Fujinami K, Sergouniotis PI, Davidson AE, et al. The clinical effect of homozygous ABCA4 alleles in 18 patients. *Ophthalmology*. 2013;120:2324–2331.
22. McCulloch DL, Marmor MF, Brigell MG, et al. ISCEV Standard for full-field clinical electroretinography (2015 update). *Doc Ophthalmol*. 2015;130:1–12.
23. Lois N, Holder GE, Bunce C, Fitzke FW, Bird AC. Phenotypic subtypes of Stargardt macular dystrophy-fundus flavimaculatus. *Arch Ophthalmol*. 2001;119:359–369.
24. Robson AG, Webster AR, Michaelides M, et al. "Cone dystrophy with supernormal rod electroretinogram": a comprehensive genotype/phenotype study including fundus autofluorescence and extensive electrophysiology. *Retina*. 2010;30:51–62.
25. Neveu MM, Dangour A, Allen E, et al. Electroretinogram measures in a septuagenarian population. *Doc Ophthalmol*. 2011;123:75–81.
26. Genead MA, Fishman GA, Stone EM, Allikmets R. The natural history of stargardt disease with specific sequence mutation in the ABCA4 gene. *Invest Ophthalmol Vis Sci*. 2009;50:5867–5871.
27. Duncker T, Tsang SH, Woods RL, et al. Quantitative fundus autofluorescence and optical coherence tomography in PRPH2/RDS- and ABCA4-associated disease exhibiting phenotypic overlap. *Invest Ophthalmol Vis Sci*. 2015;56:3159–3170.
28. Fujinami K, Sergouniotis PI, Davidson AE, et al. Clinical and molecular analysis of Stargardt disease with preserved foveal structure and function. *Am J Ophthalmol*. 2013;156:487–501, e481.
29. Noupuu K, Lee W, Zernant J, Tsang SH, Allikmets R. Structural and genetic assessment of the ABCA4-associated optical gap phenotype. *Invest Ophthalmol Vis Sci*. 2014;55:7217–7226.
30. Weng J, Mata NL, Azarian SM, Tzekov RT, Birch DG, Travis GH. Insights into the function of Rim protein in photoreceptors and etiology of Stargardt's disease from the phenotype in abcr knockout mice. *Cell*. 1999;98:13–23.
31. Mullins RF, Kuehn MH, Radu RA, et al. Autosomal recessive retinitis pigmentosa due to ABCA4 mutations: clinical, pathologic, and molecular characterization. *Invest Ophthalmol Vis Sci*. 2012;53:1883–1894.
32. Bonilha VL, Rayborn ME, Bell BA, Marino MJ, Fishman GA, Hollyfield JG. Retinal histopathology in eyes from a patient with Stargardt disease caused by compound heterozygous ABCA4 mutations. *Ophthalmic Genet*. 2014;1–11.
33. Biswas-Fiss EE, Affet S, Ha M, Biswas SB. Retinoid binding properties of nucleotide binding domain 1 of the Stargardt

Investigative Ophthalmology & Visual Science

disease-associated ATP binding cassette (ABC) transporter ABCA4. *J Biol Chem*. 2012;287:44097–44107.

34. Sabirzhanova I, Lopes-Pacheco M, Rapino D, et al. Rescuing trafficking mutants of the ATP binding cassette protein, ABCA4, with small molecule correctors as a treatment for Stargardt eye disease. *J Biol Chem*. 2015;290:19743–19755.
35. Wang XR, Li C. Decoding F508del misfolding in cystic fibrosis. *Biomolecules*. 2014;4:498–509.
36. Clancy JP, Rowe SM, Accurso FJ, et al. Results of a phase IIa study of VX-809, an investigational CFTR corrector compound, in subjects with cystic fibrosis homozygous for the F508del-CFTR mutation. *Thorax*. 2012;67:12–18.

Investigative Ophthalmology & Visual Science